Charakterisierung des Kriechverhaltens von Kraftaufnehmern
Characterizing the creep response of load cells

Von **R. A. Mitchell/S. M. Baker**, Washington D. C./USA

A procedure is being developed for characterizing the creep response of load cells. A constant force is applied to the load cell in a dead weight machine and the creep response is recorded using a high precision direct-current indicator. Initial test results on eleven strain-gage load cells indicate a great variety in the magnitude, direction and complexity of creep and creep recovery.

A rheological model consisting of multiple spring and dashpot elements in parallel and in series is fitted to the creep data. A search algorithm is used to solve the nonlinear least squares problem for the multiple stiffness and time constants of the rheological model. Within the limitations imposed by nonlinearity in the creep response, the fitted model can be used to estimate the creep response due to more general loading.

Es wurde ein Verfahren entwickelt, um das Ansprechverhalten von Kraftaufnehmern auf Kriechdehnung zu kennzeichnen. Auf den Kraftaufnehmer wird in einer Bealstungsmaschine mit unmittelbarer Massewirkung eine konstante Kraft eingeleitet, und mit Hilfe eines Präzisionsgleichstromindikators wird das Ansprechverhalten auf Kriechdehnung aufgezeichnet. Anfangstestergebnisse an elf mit Dehnungsmeßstreifen versehenen Kraftaufnehmern zeigen eine große Variationsbreite in bezug auf Größe, Richtung und Komplexität der Kriechdehnung und ihrer Restitution an.

Ein Fließmodell, das aus Mehrfachfederelementen und Dämpfungszylinderelementen besteht, parallel geschaltet und mit Reihenschaltung versehen, wird den Kriechdehnungsdaten angepaßt. Ein Suchalgorithmus wird verwendet, um das nichtlineare Problem kleinster Quadrate für Vielfachsteife und für Zeitkonstanten des Fließmodells zu lösen. Das angepaßte Modell kann zur Errechnung des Ansprechverhaltens auf Kriechdehnung - innerhalb der durch die Kriechdehnung verursachten Nichtlinearitätsgrenzen - für einen allgemeinen Belastungsfall verwandt werden.

1. Introduction

Load cell creep can equal from 0.01 to 0.1 percent of rated output and it is quite systematic. Therefore, it is worth correcting for in such applications as precision mass comparisons and in studying other sources of error such as non-symmetrical loading. Also, creep should be considered in selecting the preloading, calibration loading, and data logging sequence of a load cell calibration procedure.

Load cell creep is defined here to be the change in load cell output that takes place after the initial response to the force increment, excluding any transient inertial response caused by the force increment. To appreciate the complexity of the creep response, it is useful to consider a load cell as a system of elements, with each element involved in a combination of creep processes. A strain-gage load cell consists of a primary load supporting element, other elements that may partially support the load (such as diaphragms, covers and the gas enclosed by them), strain gages and adhesives, precision resistors, lead wires, and threaded connections or bearing surfaces. When load is applied to a load cell there is an initial deformation of all constituent stressed material, followed by a delayed creep deformation of the material. There is also an initial change in temperature of all deformed material, followed by a delayed temperature change as the elements approach a new thermal equilibrium state. The temperature changes cause additional changes in the dimensions of the elements and also changes in their elastic and electrical properties. Clearly, load cell creep involves a complex combination of several interrelated time dependent processes. This situation suggests that a direct empirical study of the response of the

load cell system as a whole is, at present, the most appropriate method of characterizing load cell creep.

2. Test Procedure

The procedure was to apply a constant force to the load cell in a dead weight machine and to record the electrical output over a period of from one hour to several days using a high precision DC indicator. The force was then removed and the creep recovery was similarly recorded. The maximum loading rates available in the respective dead weight machines were used to approximate step function loading. The test loads applied by these machines and the corresponding times required to apply and remove the test loads are given in T a b l e 1.

Table 1. Loading and Unloading Times in Dead Weight Machines

Test Loads		Loading Time	Unloading Time
(newtons)	(pounds-force)	(seconds)	(seconds)
4 448 200	1 000 000	331.0	529.0
444 820	100 000	24.0	48.0
222 410	50 000	2.4	9.0
111 210	25 000	0.8	0.9
88 964	20 000	15.0	22.0
44 482[1])	10 000	1.6	2.3
44 482[1])	10 000	0.5	0.3
11 121	2 500	2.7	2.2

[1]) Two different machines used for this load level.

The DC indicator was read and recorded by hand to one part per million counts of load cell rated output. The stability of the zero and span settings of the indicator were checked several times during a test using a well characterized, stable, step-variable, four terminal resistance network. The linearity and long term stability of the indicator were checked several times during the testing program using the same four terminal network. An electrical excitation of 10 volts was applied to the load cell input terminals.

Air temperature is controlled at 23 $\pm$ 0.5°C in the laboratory. Barometric pressure was recorded during most of the tests because some load cells respond significantly to changes in air pressure. A rough calibration of the air pressure sensitivity of most of the load cells was obtained by recording the barometric pressure and the corresponding (unloaded) load cell output at convenient times over a period of several weeks. Linear fits of this data (plotted as percent of rated output versus barometric pressure) for two load cells are shown in F i g u r e 1. During the several months of this testing program the barometric pressure in

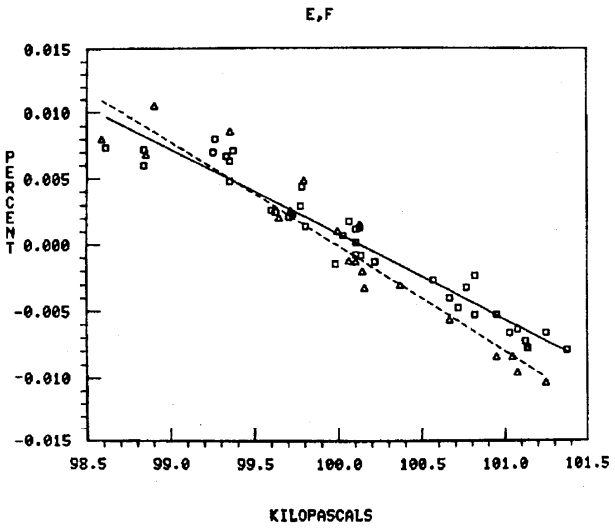

Fig. 1. Air pressure sensitivity of two load cells of 44 482 N (10 000 lbf) rated capacity.

the laboratory ranged over 5.7 kPa, enough to account for an error of about 0.045 percent of rated capacity in one of the load cells represented in F i g u r e 1. Where barometric pressure data was available, the recorded creep test data was corrected for this effect.

3. Test Results

Eleven different load cells were creep tested. Three were designed and made at NBS for use as force transfer standards. The remaining eight were commercially produced. F i g u r e s 2 through 9 are normalized plots of the creep and creep recovery data obtained from the tests. The normalized electrical output of the load cell, in percent of rated output, is given by the vertical scale. Increasing magnitudes of load cell output correspond to algebraically increasing creep values plotted on this scale. The time elapsed after application or removal of the test load is given by the horizontal scale. The plots have been normalized by subtracting the output (interpolated) at 60 minutes from the recorded output, thus forcing the plotted output through zero percent at 60 minutes without distorting the shapes of the plots. Where solid or dashed curves are shown, they were developed by connecting adjacent data points.

The creep and creep recovery plots (F i g u r e s 2 through 9) indicate a wide range of creep characteristics for the eleven load cells tested. In most cases where tests were repeated, there is good agreement between the data (F i g u r e s 2, 3 and 4). In most cases there is at least a qualitative

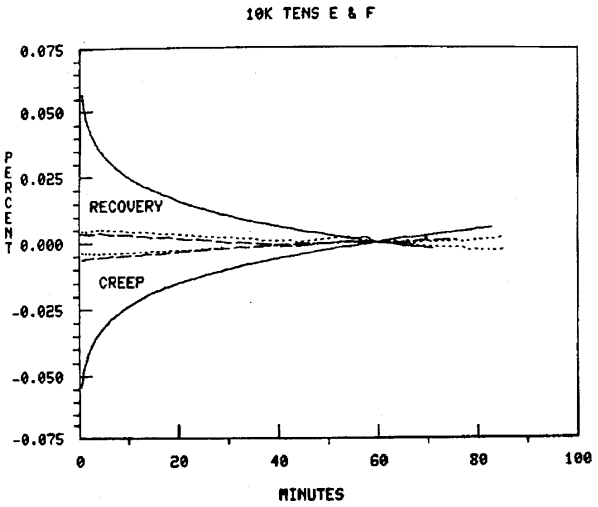

Fig. 2. Creep response of two universal load cells of 44 482 N (10 000 lbf) rated capacity loaded to rated capacity in tension.

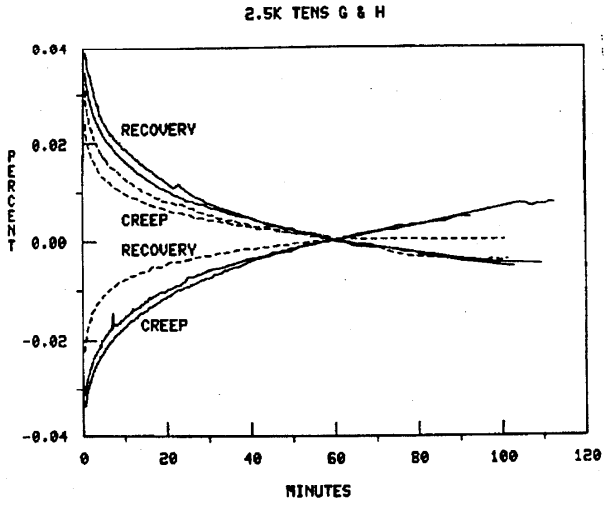

Fig. 3. Creep response of two universal load cells of 11 121 N (2 500 lbf) rated capacity loaded to rated capacity in tension.

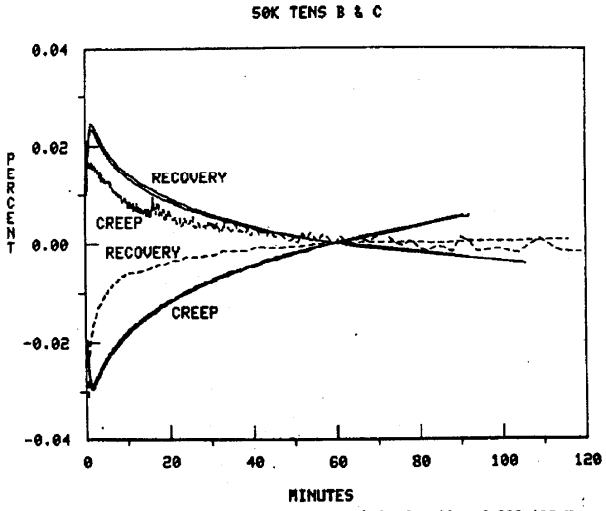

Fig. 4. Creep response of two universal load cells of 222 410 N (50 000 lbf) rated capacity loaded to rated capacity in tension.

symmetry between the creep and creep recovery curves (F i g u r e s 2, 3, 4, 5, 7, 8 and 9). In contrast, the plots for compression creep tests of two similar NBS produced load cells (F i g u r e 6) indicate less repeatability and no apparent symmetry. This may be related to inelastic deformation and radial friction slip of the bearing blocks used to apply the compressive load to the spherical upper end of these load cells. One would expect some variability and irreversibility in these inelastic deformation and friction processes. An earlier analytical and experimental study of compression load cells conducted at NBS [1] demonstrated the sensitivity of load cell output to variations in the distribution

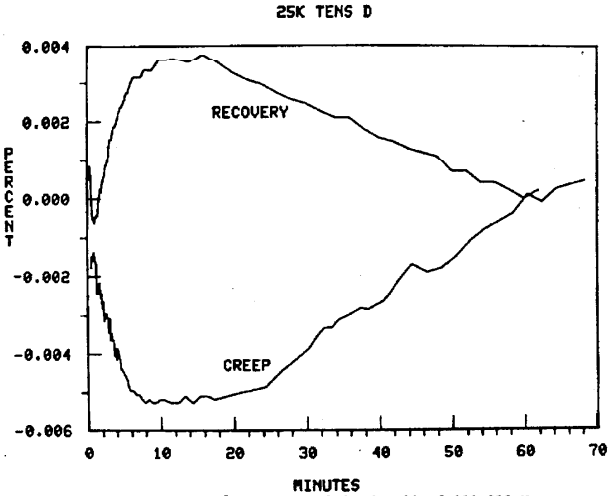

Fig. 5. Creep response of a universal load cell of 111 210 N (25 000 lbf) rated capacity loaded to rated capacity in tension.

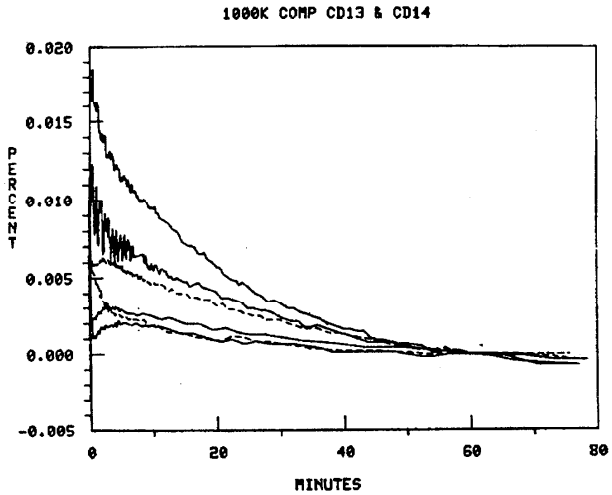

Fig. 6. Creep response of two similar compression load cells of 4 448 200 N (1 000 000 lbf) rated capacity loaded to rated capacity. The two upper solid curves are creep plots from repeated tests on one load cell; the two lower solid curves are creep recovery plots from these tests. The upper dashed curve is the creep recovery plot for the other load cell, and the lower dashed curve is the creep plot.

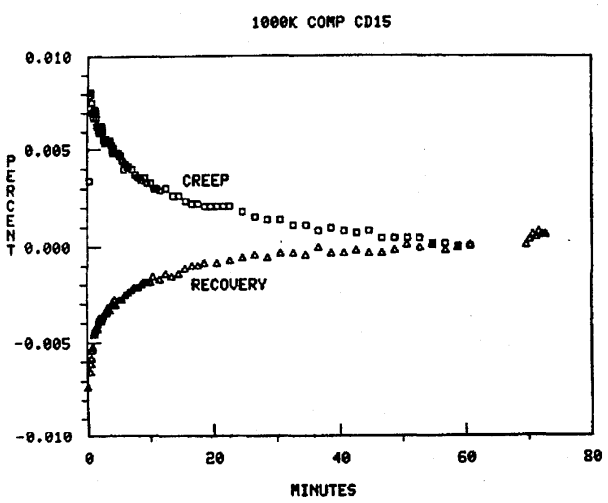

Fig. 7. Creep response of a compression load cell of 13 345 000 N (3 000 000 lbf) rated capacity loaded to 4 448 200 N (1 000 000 lbf).

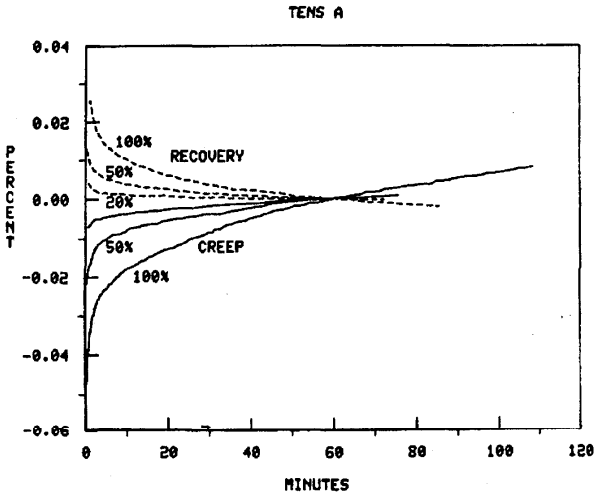

Fig. 8. Creep response of a universal load cell of 444 820 N (100 000 lbf) rated capacity loaded to 100, 50 and 20 percent of rated capacity in tension.

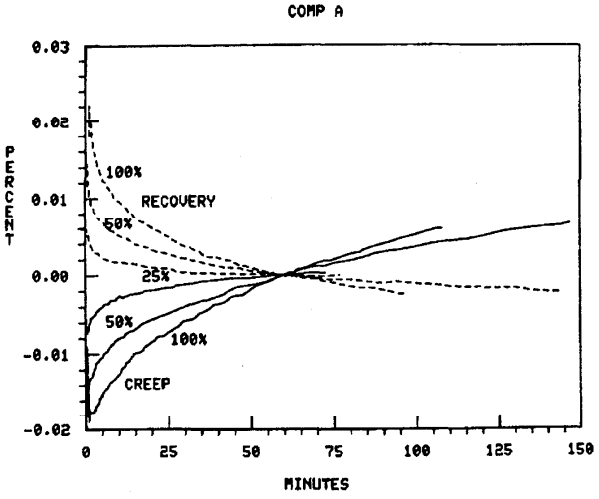

Fig. 9. Creep response of a universal load cell of 444 820 N (100 000 lbf) rated capacity (the same load cell as in Figure 8) loaded to 100, 50 and 25 percent of rated capacity in compression.

of contact stresses at the bearing surfaces. The third NBS produced load cell was tested at only one-third of rated capacity and the resulting plot shows a qualitative symmetry (Figure 7). At that load level inelastic deformation and friction slip of the bearing blocks are much less than at rated capacity load.

A reversal in the direction of the creep response is clearly evident during the first few minutes of the repeated tests shown in Figure 4. There are two such reversals evident in Figure 5, one during the first 2 minutes and another between 10 and 20 minutes. These reversals suggest the dominance of different creep mechanisms of different sign, magnitude and time constant during different stages of the test. The dominant creep responses are in opposite directions for the two cases shown in Figure 3, and also for the two shown in Figure 4.

The creep response to different levels of tension and compression loading shown in Figures 8 and 9 suggests a rough linearity of response with load level. This question was studied by the following analysis.

4. Rheological Model Analysis

In order to get a quantitative understanding of the results shown in Figures 8 and 9, a rheological model was fitted to the data. Such rheological models have been used to study the creep of solid materials (see, for example, [2]). The particular model used in the present analysis was the idealized network of springs and dashpots shown in Figure 10. In comparing the rheological model with the load cell, the displacement of point 0 relative to point 1 (Figure 10) corresponds to the instantaneous output of the load cell due to the application of a load increment. The displacement of point 1 relative to point n corresponds to the creep output of the load cell.

The elongation of each spring in the model is defined by an equation of the form

$$\delta = \frac{F}{E} \qquad (1)$$

in which F is the force acting on the spring and E is the stiffness constant of the spring. The elongation of each dashpot is defined by an

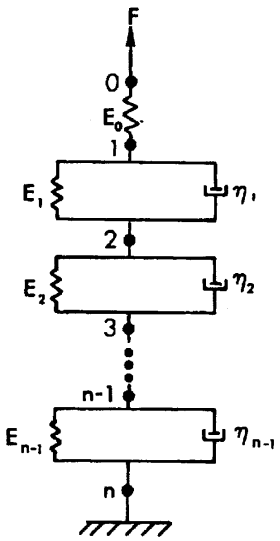

Fig. 10. Spring and dashpot rheological model.

equation of the form

$$\frac{d\delta}{dt} = \frac{F}{\eta} \qquad (2)$$

in which F is the force acting on the dashpot, t is the time variable, and η is the elongation-rate constant of the dashpot. In the combination of a spring and a dashpot in parallel, called a Voigt element, each experience the same elongation, δ, and the sum of the forces acting on the spring and dashpot equals the force acting on the Voigt element. The elongation of a Voigt element is defined by a linear differential equation with constant coefficients of the form

$$\eta \frac{d\delta}{dt} + E\delta = F \ . \qquad (3)$$

This Voigt element is linear in the sense that it obeys the Boltzmann superposition principle. That is, the elongation resulting from a linear combination of loads is the linear combination of the elongations due to each of the loads individually. If a force is applied to a Voigt element as a step function, the elongation of the element is given by the following solution to Equation 3:

$$\delta = \frac{F}{E}\left(1 - e^{-\frac{E}{\eta}t}\right) \qquad (4)$$

For elements combined in series, as in F i g u r e 10, the total elongation of the series due to a step loading function equals the sum of the element elongations, or

$$\delta = \frac{F}{E_0} + F\left[\left(\frac{1}{E_1} - \frac{1}{E_1}e^{-\frac{E_1}{\eta_1}t}\right) + \ldots + \left(\frac{1}{E_n} - \frac{1}{E_n}e^{-\frac{E_n}{\eta_n}t}\right)\right] \qquad (5)$$

Admittedly, the step loading function assumed in Equation 5 is only approximated by the test loading rates indicated in T a b l e 1, and inertial effects are not represented in the rheological model.

An optimization search algorithm [3] was used to solve the nonlinear least squares problem of fitting Equation 5 to the test data. Single exponential curves (n = 1 in Equation 5) were first fitted to

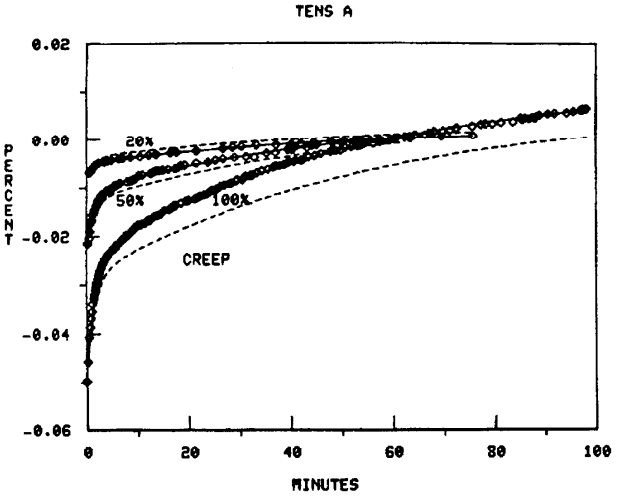

Fig. 11. Three double exponential fits to tensile creep data for case shown in F i g u r e 8. Fits are plotted as solid curves through data. Dashed curves are computed using mean values of constants from the three fits.

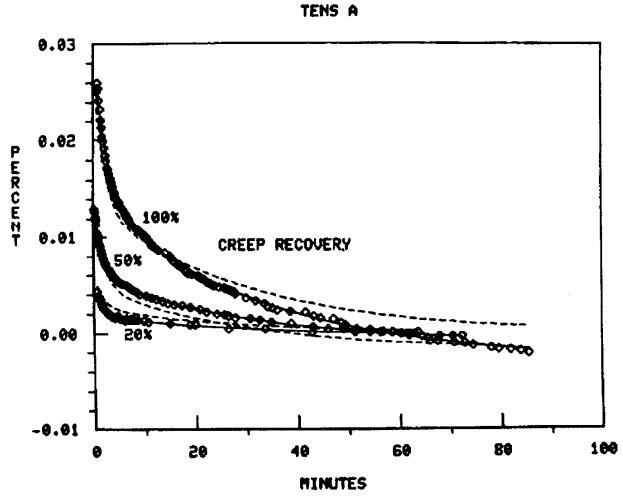

Fig. 12. Three double exponential fits to tensile creep recovery data for case shown in F i g u r e 8. Fits are plotted as solid curves through data. Dashed curves are computed using mean values of constants from the three fits.

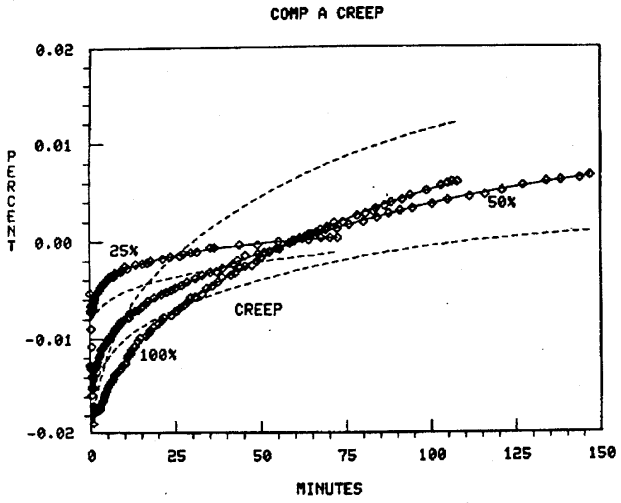

Fig. 13. Three double exponential fits to compression creep data for case shown in F i g u r e 9. Fits are plotted as solid curves through data. Dashed curves are computed using mean values of constants from the three fits.

some of the data in F i g u r e 8, but the agreement with the test data was relatively poor. Double exponential fits were then obtained with the tension creep and creep recovery data and with the compression creep data, and the results are shown in F i g u r e s 11, 12, and 13. The solid curve running through each set of data points is the fitted curve for that particular set of points. The four constants (E_1, E_2, η_1, η_2) defining each fitted curve in F i g u r e 11 were then averaged and the mean values were used in Equation 5 to compute the dashed curves. The constants defining each fitted curve in F i g u r e s 12 and 13 were similarly averaged and the mean values were used to compute the dashed curves. Although the dashed curves diverge from the data, these results suggest that creep data obtained at one or more load levels may be useful in predicting the creep response at other load levels, providing the loads are applied in the same direction.

5. Conclusion

The results of tests on eleven different load cells indicate a wide variety in the magnitude, direction, and complexity of the creep response. This is not surprising if one considers the variety of interrelated mechanical, thermal and electrical processes involved as the load cell system creeps toward an equilibrium state.

The rheological model analysis is a useful means of quantifying the creep characteristics of a load cell. For the one load cell compared with this model, double exponential curves fitted the separate sets of data points (representing single creep or creep recovery tests) very well. Additional exponential terms would probably be needed to characterize some load cells or to characterize creep response over a longer time. In using a rheological model to predict creep response to a loading sequence not represented by the fitted data, one should take into account the nonlinearity of the particular load cell.

References

[1] Mitchell, R.A., Woolley, R.M., Fisher, C.R., Formulation and experimental verification of an axisymmetric finite-element structural analysis, J. Res. NBS 75C, July-Dec. 1971, pp. 155-163.

[2] McClintock, F.A., Argon, A.S., editors, Mechanical Behavior of Materials, (Addison-Wesley, Inc., 1966), pp. 243-253.

[3] Mitchell, R.A., Kaplan, J.L., Nonlinear constrained optimization by a nonrandom complex method, J. Res. NBS 72C, Oct.-Dec. 1968, pp. 249-258.